参赛学生姓名：李弘毅

中　学：中国人民大学附属中学

省　份：北京市

指导老师单位：北京化工大学

国家/地区：中　国

指导老师姓名：杨志宇

论文题目：基于增强 Mn-O 键原理的高稳定超级电容器二氧化锰电极材料研究

Strengthen Mn-O bonding to Construct Super Stable Manganese Dioxide Electrode Materials for Supercapacitor

Author: Hongyi Li

High school: The High School Affiliated to Renmin University of China, Beijing, China

Instructor: Professor Zhiyu Yang

Beijing University of Chemical Technology

September, 2024

Abstract:

Supercapacitors have been playing an increasingly important role in energy storage technology. Manganese dioxide (MnO_2) is regarded as the promising candidate electrode material to address low energy density issue for supercapacitors due to its high theoretical capacitance and high natural abundance. However, MnO_2 suffers from inferior cycling stability induced by irreversible structural degradation and Mn ions dissolution during the charge and discharge process. Herein, the strengthening Mn-O bonding strategy is proposed through F relacing O to suppress structure distortion and Mn ions dissolution. Theoretical calculations indicate that the electron interaction increases between Mn and O atoms owing to F incorporation, resulting in strengthened Mn-O bond. Meanwhile, the band gap and sodium ion adsorption energy are reduced, which facilitated electron transfer and sodium ion adsorption. Experiments further demonstrate that strengthened Mn-O bond due to F introduction significantly enhances cycle life of MnO_2 electrode materials from capacity retention rate of 19.34% to 82.52% after 20,000 cycles. Additionally, F-MnO_2 achieves a higher special capacity of 414.6 F g^{-1} at 0.5 A g^{-1} than that of 273 A g^{-1} of MnO_2 as electrode material. This work reveals the enhanced mechanism of strengthening Mn-O bond on cycle stability of MnO_2 electrode materials, and provides a methodical approach for constructing the ultra-long cycle life manganese oxide electrode materials.

Keywords: Supercapacitor, Electrode materials, Manganese Dioxide, Cycle stability

Table of Contents

1 Introduction

With the increasing consumption of fossil energy and the aggravated harm of environmental pollution, it is necessary to develop renewable energy storage devices with fast charge and discharge speed and high efficiency. Supercapacitors (SCs) have been attracting much attention owing to their high power density and high safety and playing an important role for developing electric vehicles, wearable devices and large-scale energy storage [1]. In addition, supercapacitors are irreplaceable for short-time power compensation when there are transient disturbances and sudden power changes in the power grid, and stability regulation when there are frequency and voltage instabilities in wind power and solar energy generation. Although they can achieve short-time power compensation when applied in electric vehicles and large-scale energy storage systems, they still suffer from low energy density [2]. As an integral part of modern energy storage devices, it is urgent to improve their energy storage performance for widespread applications. Constructing electrode materials with excellent electrochemical performance is the key to achieve a further breakthrough in next-generation supercapacitors remaining high energy density and power density [3].

Intensive endeavors have been devoted to develop advanced cathode materials for supercapacitors, including graphene, MXene, metal oxides, sulfides, carbides, etc. [4-8]. Among them, manganese dioxide (MnO_2) has attracted considerable attention due to its high theoretical capacitance (1380 F g^{-1}), high natural abundance, low cost and environmental friendliness, which is regarded as promising cathode material for supercapacitors. However, MnO_2 suffers from inferior cycling stability induced by irreversible structural evolution and Mn ions dissolution during the charge and discharge process [9,10].

Recently, numerous methods have been employed to address these issues, including defect engineering, pre-embedding method, constructing new structure and morphology and doping strategy [11]. Defect engineering involving in oxygen vacancies, metal ion vacancies and double vacancies, as an effective technology to change the intrinsic electronic structure of materials, provide more active sites to participate in the

charge/discharge process and increasing capacity for the electrode material [12]. Pre-embedding method is to prevent lattice changes through pre-inserting ions or molecules as pillars and endow MnO_2 with large interlayer spacing, resulting in fast diffusion kinetics [13]. Constructing distinctive morphology can increase the specific surface area and facilitate ion transfer. Therefore, in order to enrich the morphology and structure of MnO_2, various morphologies such as nanorods, nanowires, nanofibers, nanotubes, nanobelts, nanosheets and nanoflowers have been developed. In addition, hollow structure, ultrathin structure, and 3D network structure are controlled to enhance energy storage performance of MnO_2. Doping strategy is regarded as an important strategy to improve cycle stability and ion adsorption capability of MnO_2. The metal and non-metal elements doping can restrain the bond length, optimize electronic structure and enhance orbital hybridization, thereby suppressing construct degradation and improving capacity. Although the introduction of these modification methods alleviates the capacity attenuation during the cycling process and effectively improves the performance of MnO_2, severe capacity loss of MnO_2 during cycle process has not been effectively solved, resulting in low cycle life of MnO_2, which becomes a bottleneck restricting practical application of MnO_2 as the energy storage electrode material.

The main reason for the capacity loss of MnO_2 is the synergy effect between structural degradation and Mn dissolution [14]. During the charge-discharge process, the insertion and extraction of ions cause irreversible structural distortion, which accelerates severe manganese dissolution. Meanwhile, the rapid dissolution of manganese triggers irreversible structural degradation. Essentially, structural degradation and Mn dissolution is relative to the Mn-O bonding. The weak bonding between Mn and O is easily to be broken in the process of the insertion and extraction of ions, resulting in Mn ions migrate and dissolve into the electrolyte. Consequently, fragility of manganese-oxygen bond causes low cycle stability. Therefore, it can be inferred that establishing the strong bonding between Mn ion and O ions is beneficial to achieve the ultra-long cycle life of MnO_2.

In this report, we proposed a strategy to strengthen Mn-O bonding for enhancing

cycle stability of MnO_2 electrode materials. A feasible F doping approach was applied to examine this strategy. DFT calculations indicated that Mn-O bond was strengthened and the distance between Mn and O was reduced due to F incorporation, which is beneficial to suppress structure distortion and Mn ion dissolution. Meanwhile, the band gap and sodium adsorption energy were decreased, facilitating electrons transfer and ion adsorption. Experiments further elucidated that cycle stability enhances and the capacity retention increases from 19.34% to 82.52% after 20,000 cycles. Additionally, a higher special capacity of 414.6 F g^{-1} at 0.5 A g^{-1} than a special capacity of 273 A g^{-1} of MnO_2 as electrode material was achieved. The results demonstrated that high cycle stability of MnO_2 electrode materials can be achieved through reinforcing Mn-O bond, F-doping is a feasible method to strengthen Mn-O bonding.

2 Materials and methods

2.1 Materials and instruments

$KMnO_4$, $MnSO_4$ and MnF_2 were purchased from Guangdong Engineering Technology Research, Shanghai Macklin Biochemical Technology Co., Ltd. and Aladdin Reagent (Shanghai) Co., Ltd., respectively. Alcohol was purchased from Shanghai Macklin Biochemical Technology Co., Ltd. N-methylpyrrolidone(NMP) and Polyvinylidene fluoride (PVDF) were obtained in Aladdin (Shanghai) Biochemical Technology Co., Ltd. Acetylene black was from Suzhou Jilongsheng Energy Technology Co., Ltd. Carbon paper was obtained from Beijing Jinglong Special Carbon Technology Co., Ltd. All above reagents were used directly without further treatment or purification. Deionized water was obtained from purified water equipment in the Lab.

All instruments used in experiments include: analytical balance(Me104, Mettler), magnetic stirrer (ZNCL-DLB140*140, Shanghai Biaohe Instrument Co.,Ltd.), electrochemical workstation (Chi660E, Shanghai Chenhua Instrument Co.,Ltd.), vacuum drying oven (DZF-6020, Shanghai Biaohe Instrument Co.,Ltd.), high speed centrifuge (MG 1650, Meric Instrument Co., Ltd.), the scanning electron microscopy (SEM, Zeiss GeminiSEM 360), high-resolution transmission electron microscopy(HRTEM, FEI Talos F200x), X-ray photoelectron spectroscopy (XPS,

Thermo Scientific ESCALAB 250Xi) , X-ray diffraction (XRD, Ultima IV).

2.2 Materials synthesis and electrodes preparation

Figure 1 shows the synthesis process of F doping MnO_2(F-MnO_2) via one-step hydrothermal method, and the fluorination process was carried out in hydrothermal method. Initially, $KMnO_4$ and $MnSO_4$ were mixed at a molar ratio of 1:6, and MnF_2 as the F source was added at a mass ratio of 5%. Secondly, the mixture was dissolved in 50 ml deionized water and stirred 1h, and then moved into a hydrothermal reactor. The reaction temperature was controlled at 120◦C for 12 hours. Finally, the reactants were centrifugally filtered under room temperature, washed with deionized water and ethanol, and the precipitate was dried for 12 hours and collected, denoted as F-MnO_2. For comparison, pure MnO_2 was synthesized under the same method and conditions.

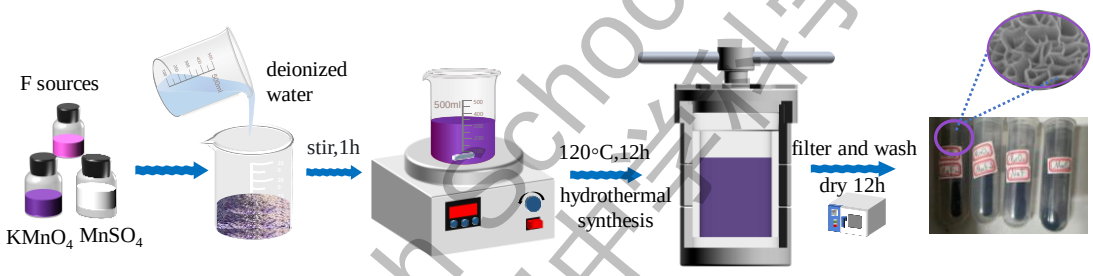

Figure 1 The synthesis process of F-MnO_2

Electrodes were prepared by coating the slurry of prepared samples on the carbon paper. The prepared active material, acetylene black and PVDF were weighted at a ratio of 8:1:1 and dissolved in 1 ml of NMP. Subsequently, the slurry was stirred until the mixture was completely dissolved. The well-stirred slurry was coated on the 1 cm^2 carbon paper with a pipette. The carbon paper coated slurry was dried for 12 h at 60 °C to evaporate the solvent in an oven. The resulting working electrode can be used for electrochemical measurement.

2.3 Material characterization

The microstructure and morphology were characterized by SEM and HRTEM. F incorporation and elemental distribution of the as-prepared samples were analyzed through energy-dispersive X-ray spectroscopy (EDS) mapping images. XPS spectra was performed to reveal the surface electronic structure and composition information

of the as-synthesized samples. The crystal structure is characterized by XRD patterns.

2.4 Electrochemical measurements

Electrochemical measurements were performed in a three-electrode system in 1.0 M Na_2SO_4 aqueous electrolyte, as showed in Figure 2. The as-prepared electrode with active materials was used as the working electrode, the Ag/AgCl electrode was taken as the reference electrode, and the platinum electrode was acted as the counter electrode. All electrodes were placed in electrolyte cell with Na_2SO_4 electrolyte. Cyclic voltammetry (CV), galvanostatic charge discharge (GCD) and electrochemical impedance spectroscopy (EIS) measurements were conducted within a potential window of 0 to 1.0 V to evaluated the electrochemical properties of the electrode. The electrochemical workstation CHI 660E was used for above electrochemical measurements.

Figure 2 Electrochemical measurement method

2.5 Computational details

Density functional theory (DFT) calculations were performed on different theoretical models through VASP software. In the calculation process of this work, the plane wave pseudopotential technique is adopted, and the PBE functional (Perdew-Burke-Ernzerhof functional) in the generalized gradient approximation (GGA) was used to simulate the electron exchange correlation function. The ion and electron interaction was calculated through the projection augmented wave (PAW) pseudopotential. Meanwhile, a cut-off energy of 520 eV is set for plane wave expansion, and a 20 Å vacuum layer was added in the z-axis direction of each model to effectively eliminate the interaction due to periodicity between adjacent images. The calculation formula for adsorption energy is as follows:

$$E_{ads} = E_{total} - E_{material} - E_{ion}$$

Here, E_{total} represents the total energy of material adsorbing Na^+, $E_{material}$ is the energy of material without adsorbing Na^+, E_{ion} describes the energy of Na^+.

3 Results and Discussion

3.1 Proposed Strategy

To suppress Mn dissolution and structure distortion, it is desirable to restrict Mn ions from leaving MnO_2 frame and control Mn-O bond to resist lattice distortion. Given that enhancing the Mn-O bond energy through modulating electronic structure is probably an effective strategy. The strong Mn-O bond is less prone to breakage, hence dramatically restricting Mn ion dissolution and resisting lattice distortion. Driven by this inspiration, the method of F substituting for some O atoms in MnO_2 lattice can be applied to achieve strong Mn-O bond. Among possible dopants for MnO_2, F possesses the highest electronegativity. It can be expected that the introduction of F can exhibit considerable electronic interaction with surrounding ions and improve the cycle stability of MnO_2. In addition, F ions and O ions have similar ionic radius, which can change the original lattice structure to a minimum extent.

Accordingly, F element was chosen and introduced into the crystal lattice to construct the strong Mn-O bonding between Mn and other coordinating atoms. The schematic illustration of the strategy is showed in Figure 3. Through the strong electronic interaction between the F element and other elements, the bond energy was enhanced to stabilize manganese ions in the structure and prevent the dissolution of Mn ions. Meanwhile, the bond length was controlled to suppress structural distortion. Consequently, the cycling stability of MnO_2 during the charge and discharge cycles was achieved. Moreover, it is found that MnF_2 is usually applied as glue, which reflects the strong stability between Mn and F. Hence, we chose MnF_2 as F source to effectively realize the F doping. In brief, the strengthened Mn-O bond strategy was proposed, based on the principle, F was applied to replace O in lattice to achieve enhanced Mn-O bond through modulating electrons structure.

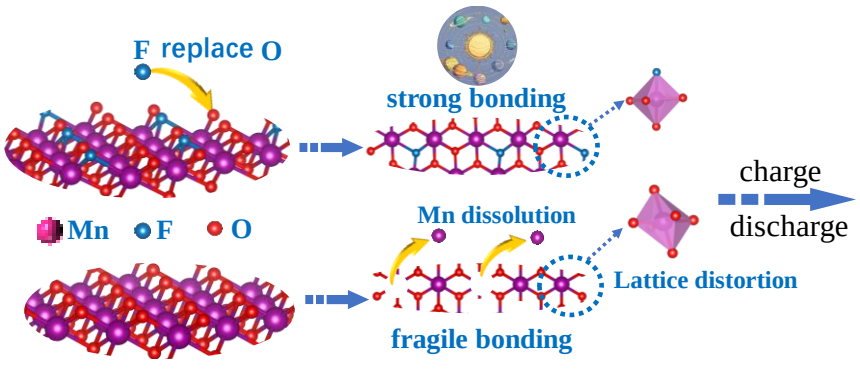

Figure 3 Schematic illustration of the strategy

3.2 Bond strength and structural stability

Guided by the proposed strategy, density functional theory (DFT) calculations were performed to predict and ascertain the role of F incorporation on the Mn-O bonding and structural stability. The model used for DFT calculations is showed in Figure 4a. Firstly, electron localization Function (ELF) was calculated to analyze electron localization distribution, the blue domain represents low electron localization while red indicates high electron localization (Figure 4b). It can be seen that the substitution of F for O increases the electron delocalization surrounding F atom and exhibits nearly free electron distribution. Meanwhile, the ELF value of the red area for O atom indicates the higher localized electron distribution than that of MnO_2 without F doping and stronger electron interaction between Mn and O atoms, leading to stronger Mn-O bonding.

Crystal Orbital Hamilton Population (COHP) calculation was applied to provide the bond properties and structural stability through analyzing the chemical bond and electronic structure interaction (Figure 4c). The COHP curve shows the chemical bond strength between different atoms [15]. The positive value represents a bonding state, and a negative value represents an antibonding state, respectively. The calculated COHP profile below the Fermi level indicates a reduction of antibonding occupied state for F-MnO_2 compare to MnO_2, which elucidates the enhanced Mn-O interactions. The further integral COHP (ICOHP) for $Mn_{(4)}$-$O_{(10)}$ was calculated to quantitively confirm the Mn-O bonding strength, as shown in Figure 4d. The heightened bond strength was obtained in F-MnO_2, which can be demonstrated by the reduced distance between Mn and O

from 1.97 Å in MnO_2 to 1.91 Å after F introduction. Consequently, the lattice distortion of MnO_2 is suppressed, which is conductive to the stability of materials (insets of Figure 4d). In conclusion, F incorporation can enhance the Mn-O bond strength and inhibit the bond length, thereby preventing lattice distortion and improve structure stability. It can be expected that the partial substitution of F for O can suppress structural degradation and Mn dissolution, subsequently improve electrochemical performance of material during the charge and discharge process.

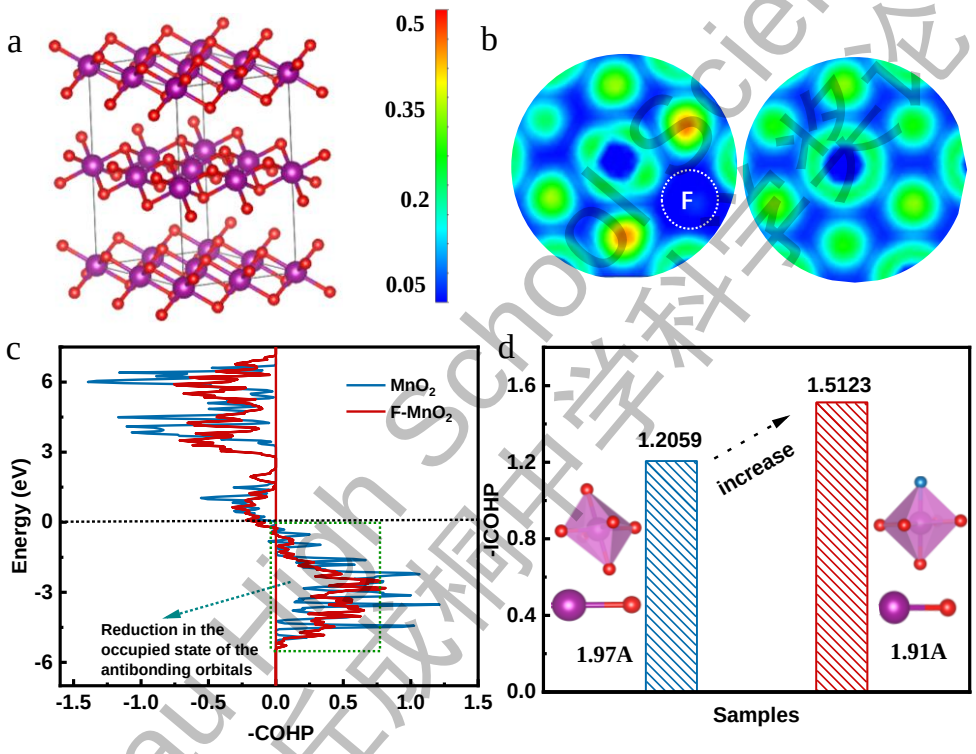

Figure 4 a) DFT calculation model for MnO_2 b) Electron localization Function (ELF) distribution of MnO_2 and F-MnO_2, c) Crystal Orbital Hamilton Population (COHP) analysis of the occupied state in MnO_2 and F-MnO_2. d) ICOHP of MnO_2 and F-MnO_2

3.3 Electronic structure and ion adsorption

To explore the mechanism of F doping on electrochemical performance of MnO_2, density of states (DOS) and differential charge density of MnO_2 and F-MnO_2 were systematically calculated to depict electronic structure and ion adsorption capability. Figure 5a depicted that total density of states of MnO_2 and F-MnO_2. It shows that the band gap between conductivity band and valence band reduces from 1.487eV of MnO_2 to 0.314 eV of F-MnO_2, indicating easier jump for electrons from valence band to

conductivity band. The reduction of band gad suggests that F introduction can enhance the electrical transfer of MnO_2. It can be illustrated from the orbital electron occupancy, as showed in Figure 5b. the introduction F 2p orbital enhance the interaction between the electrons in F 2p orbital and O 2p orbital, which leads to the shift of conductivity band. Additionally, differential charge density elucidates the feature of charge transfer (Figure 5c). The color of yellow and blue indicates an increase and a decrease in charge in charge. Compared with MnO_2 model, it shows that charge accumulation in F sites, representing electron migration from Mn to F atoms, subsequently resulting in the enhanced electron interaction between Mn and O, which reinforces Mn-O bond strength. Besides, F introduction reduces the adsorption energy of sodium ions from -3.006eV to -4.227eV, which is beneficial to enhance the adsorption capacity of sodium ions and increase the capacity of electrode materials (Figure 5d). It can be concluded that F introduction optimizes electron structure and increases ion adsorption capability.

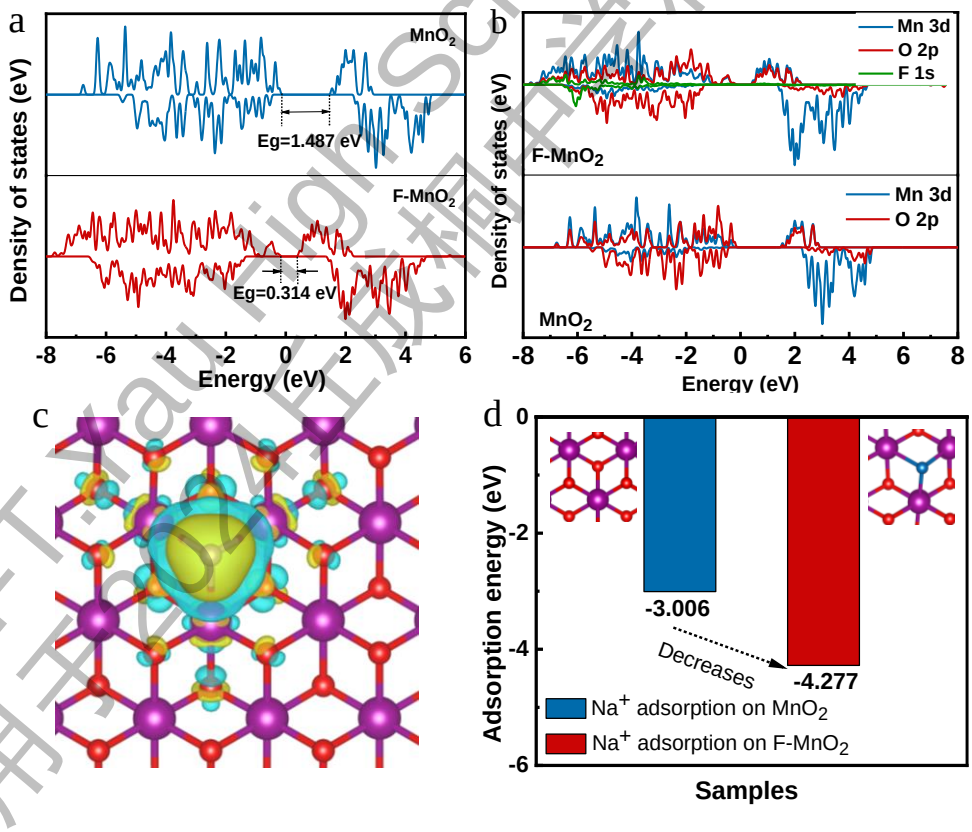

Figure 5 a) Density of state for MnO_2 and F-MnO_2. b) Partial density of states of F-MnO_2 and MnO_2. c) Electron density difference (EDD) diagram of F-MnO_2. d) The adsorption energies of Na^+.

3.4 Morphology and structures

To further demonstrate the prediction by the theoretical investigation, under theoretical guidance, we synthesized F-MnO_2 and MnO_2 via hydrothermal method, as described in Figure 1. The SEM and HRTEM images of F-MnO_2 and MnO_2 samples are showed in Figure 6. It can be seen that MnO_2 presents a nanoflower-like structure composed of stacked nanosheets (Figure 6a,b), and HRTEM clearly showed the lattice spacing is 0.619 nm corresponding to 101 plane(Figure 6.c). Compared with MnO_2 SEM images, F-MnO_2 exhibits the similar nanoflower-like structure (Figure6 d, e), the difference is that the 0.624 nm lattice space after F doping is slightly larger than that of MnO_2 (Figure 6f), possibly because of slightly larger F ionic radius. Furthermore, EDS mapping images demonstrate that F are incorporated successfully and distributed homogeneously (Figure 6 g-j). We can draw the following conclusion that MnO_2 and F-MnO_2 were prepared successfully, and the nanoflower structure is well preserved after F incorporation, which is beneficial to maintain the capacity performance of MnO_2.

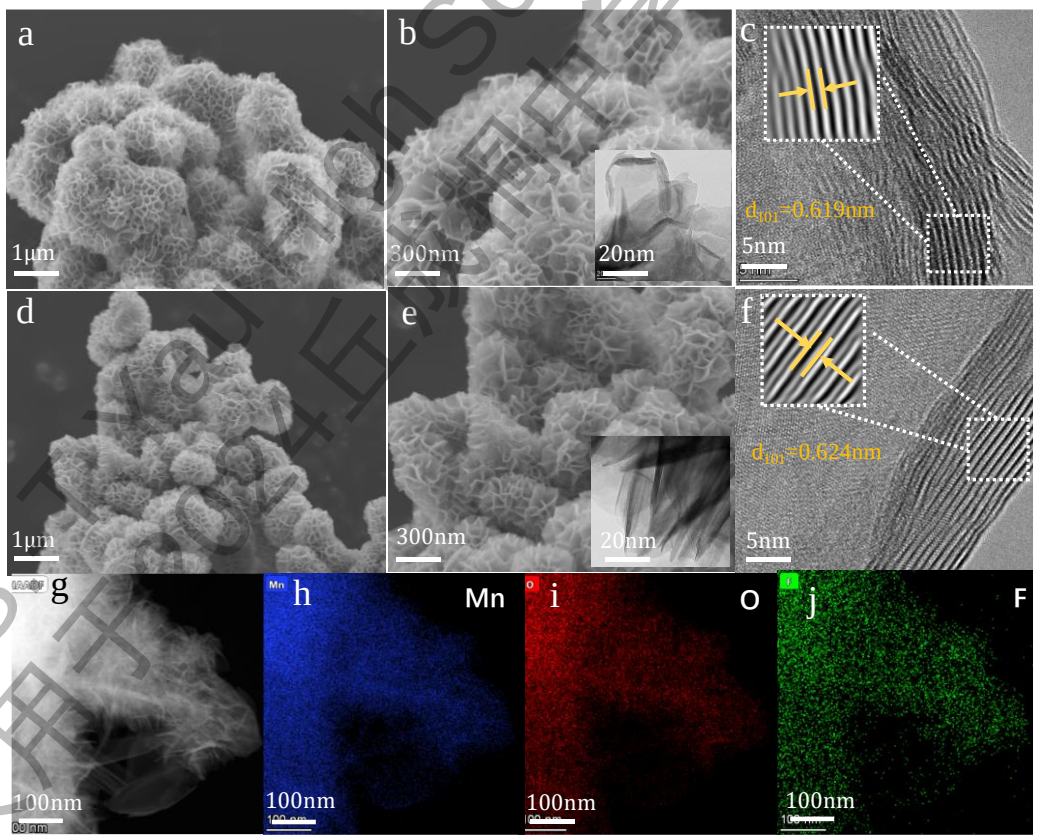

Figure 6 a), b) and c) SEM and HRTEM images of MnO_2. d), e) and f) SEM and HRTEM images of F-MnO_2. g-j) Elemental mapping images of F-MnO_2.

3.5 Chemical composition and crystal phase analysis

Figure 7a shows that the crystal structure of MnO_2 and F- MnO_2, all the diffraction peaks are indexed that of δ-MnO_2 (PDF#80-1098) without any impurity diffraction peaks, further confirming that crystal phase of MnO_2 is well preserved after F doing. In comparison with MnO_2, 001 diffraction peak appears weak and gradually shifts to higher angles, suggesting that F doing leading to a slight lattice distortion. XPS was employed to analyze the chemical composition of MnO_2 and F-MnO_2, as shown in Figure 7b. It can be seen that the elements C, Mn, O are displayed in the full spectra of MnO_2 and F-MnO_2 samples, and obvious peak of element F is observed in the full spectra of F-MnO_2 samples, indicating successful F introduction.

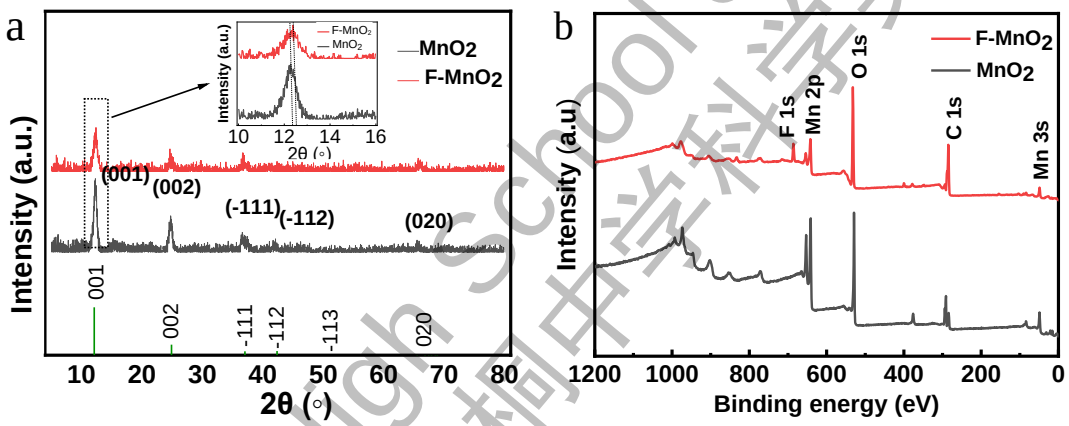

Figure 7 a) XRD patterns of MnO_2 and F-MnO_2 samples. b) XPS full spectra of MnO_2 and F-MnO_2 samples.

The characteristic peak of F1s is divided to the peaks of the absorbed F ion (684.68 eV) and the diffraction peak in F-Mn [16], the fitted peaks area of two samples further confirmed that the most of F ions are combined with Mn to form F-Mn bond, and hence replace some of lattice oxygen (Figure 8a). Two diffraction peaks of $Mn2p_{3/2}$ and Mn $2p_{1/2}$ appear in the Mn 2p spectrum plot, the fitting area ratio of Mn^{3+}/ Mn^{4+} for F-MnO_2 is 33.53%, higher than 26.85% for MnO_2, indicating some Mn^{4+} are reduces to Mn^{3+} due to F introduction into MnO_2 frame and lower the valence state of Mn ion (Figure 8b). Figure 8c shows that the lattice oxygen in F-MnO_2 is less than that of MnO_2, the fitting area ratio of $O_{lattice}/O_{defective}$ is 0.55 and 2.15 in F-MnO_2 and MnO_2 respectively, implying that F are incorporated into the frame to replace lattice O. It is concluded that

the expected F doping MnO_2 material of theoretical calculation is achieved successfully via one-step hydrothermal method and appropriate F source.

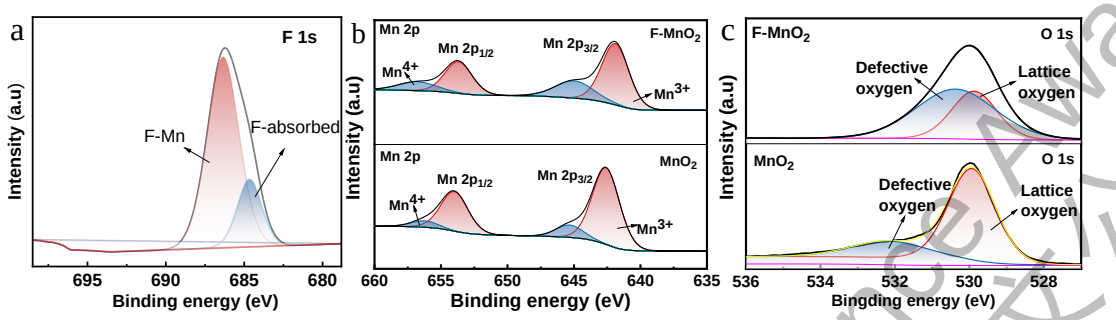

Figure 8 XPS spectra of a) F1s, b) Mn 2p, c) O1s

3.6 Electrochemical performance assessment

To explore the effect of F incorporation on the electrochemical performance, the sodium storage capabilities of the as prepared samples were evaluated using a three-electrode system (Figure 2). The cyclic voltammetry (CV) tests were carried out to examine the special capacities (Figure 9a). It indicates that two samples presented quasi-rectangular curves depicting pronounced capacitive behavior. Importantly, the integral area of F-MnO_2 surpassed that of MnO_2, indicating a larger sodium storage capability, which is consistent with the theoretical prediction. Besides, the CV curve of F-MnO_2 presents better reversibility compared to MnO_2. The GCD curves and CV curves at various scan rates further confirm this conclusion (Figure 9b,c). The GCD curve of F-MnO_2 presents more nearly ideal triangular feature than that of MnO_2, CV curves at various scan rates exhibit significantly symmetry feature, illustrating superior reversible ion intercalation and deintercalation capability during charge-discharge cycle. The excellent reversibility is beneficial to cycle stability.

Figure 9d further confirms that the enhancement of cycle stability due to the F introduction into MnO_2. It can be seen that MnO_2 presents a capacity retention rate of 19.34% after 20,000 cycles at a current density of 10 Ag^{-1}, in comparison, F-MnO_2 achieves significantly enhancement of 82.52% capacity retention rate without severe capacity loss. We can draw a conclusion that the impressive cycle performance is mainly owing to the enhanced Mn-O bonding strength, which suppress Mn dissolution and structure collapse. The electrode images of the two samples after 20,000 cycles can

manifest this conclusion (Figure 9e). It is observed that MnO_2 electrode material resulted in obvious exfoliation after long cycle, in contrast, F-MnO_2 electrode material well preserve integrity without obvious exfoliation.

Additionally, EIS tests were conducted to evaluate the charge transfer characteristic of MnO_2 and F-MnO_2, the results are showed in Figure 9f. In the high-frequency domain, no obvious semicircular shapes are exhibited in the high-frequency domain, but the fitting charge transfer resistance Rct value indicates that the conductivity of F-MnO_2 (Rct =4.544 Ω) exceeds that of MnO_2 (Rct =5.631 Ω), as predicted in theoretical calculations. In addition, the higher linear slope of the F-MnO_2 in the low-frequency area compare to that of MnO_2 suggests faster ion diffusion rate. Consequently, F incorporation effectively improves the cycle stability, and enhance conductivity and ion charge transfer rates for MnO_2 as electrode materials.

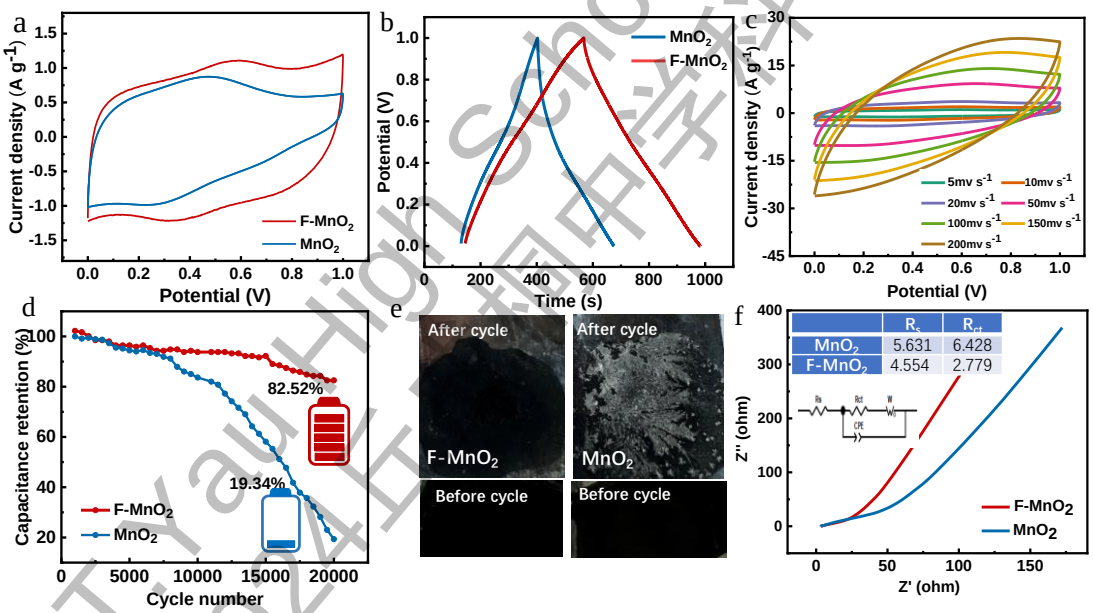

Figure 9 a) CV test in the potential window of 0 to 1.0 V at a scan rate of 5 mV s−1.b) GCD curve tested in the potential window of 0 to 1.0 V at a scan rate of 5 mV s−1. c) CV curves of F-MnO_2 at various scan rates. d) Cycle stability of MnO_2 and F-MnO_2 at at a current density of 10 A g^{-1}. e) The images of MnO_2 and F-MnO_2 before and after 20000 cycles. f) Nyquist plots of MnO_2 and F-MnO_2.

4 Conclusions

In conclusion, an effective strategy that strengthening Mn-O bonding to suppress

structure degradation and Mn ion dissolution, improving cycle stability and enhancing sodium ion adsorption capability for MnO_2 as electrodes, has been demonstrated through F introduction into MnO_2. DFT calculations indicate that F doping accelerates electrons interaction between Mn and O atoms, hence enhances Mn-O bonding. Meanwhile, F doping reduces the band gap between conductivity band and valence band to provide convenience for electron transition, and lower the sodium adsorption energy. Consequently, it is confirmed by the electrochemical experiments that the strengthened Mn-O bonding enhances cycle stability of MnO_2, the capacity retention increases from 82.52% to 19.34% after 20,000 cycles. Additionally, the reduced band gap and adsorption energy of F-MnO_2 increase the conductivity and sodium adsorption capability, achieve a higher special capacity of 414.6 F g^{-1} at 0.5 A g^{-1} than a special capacity of 273 A g^{-1} of MnO_2 as electrode material. This work reveals the mechanism of strengthening Mn-O bond, and provides a methodical approach for constructing the ultra-long cycle life manganese oxide electrode materials.

5 References

[1] Wu J, Huang F, Lee T, et al. Interface-guided formation of 2D ultrathin MnO2 nanosheets with abundant oxygen defects for high performance supercapacitors[J]. ACS Applied Energy Materials, 2022, 5(6): 6962-6969.

[2] Chen R, Tang H, He P, et al. Interface engineering of biomass-derived carbon used as ultrahigh-energy-density and practical mass-loading supercapacitor electrodes[J]. Advanced Functional Materials, 2023, 33(8): 2212078.

[3] Sammed K A, Farid A, Mustafa S, et al. Developing next-generation supercapacitor electrodes by coordination chemistry-based advanced functional carbon nanostructures: Progress, Current challenges and prospects[J]. Fuel Processing Technology, 2023, 250: 107896.

[4] Sahoo B B, Pandey V S, Dogonchi A S, et al. Synthesis, characterization and electrochemical aspects of graphene based advanced supercapacitor electrodes[J]. Fuel, 2023, 345: 128174.

[5] Kumar Y A, Raorane C J, Hegazy H H, et al. 2D MXene-based supercapacitors: A

promising path towards high-performance energy storage[J]. Journal of Energy Storage, 2023, 72: 108433.

[6] Aman S, Alahmari S D, Khan S A, et al. Hydrothermal development of bimetallic sulfide nanostructures as an electrode material for supercapacitor application[J]. Energy & Fuels, 2023, 37(22): 17473-17483.

[7] Pundir S, Upadhyay S, Priya R, et al. Synthesis of 1D β-MnO2 for high-performance supercapacitor application[J]. Journal of Solid State Electrochemistry, 2023, 27(2): 531-538.

[8] Dai Y, Gul H, Sun C, et al. Ultrafast synthesizing nanoflower-like composites of metal carbides and metal oxyhydroxides towards high-performance supercapacitors[J]. Electrochimica Acta, 2023, 438: 141575.

[9] 王绍聪, 李伟, 黄瑞琴, 等. 锰基钠离子电池正极材料 Jahn-Teller 效应抑制方法进展[J]. 储能科学与技术, 2023, 12(1): 139-148.

[10] Qu W, Cai Y, Chen B, et al. Heterointerface Engineering-Induced Oxygen Defects for the Manganese Dissolution Inhibition in Aqueous Zinc Ion Batteries[J]. Energy & Environmental Materials, 2024, 7(3): e12645.

[11] Zhang N, Ji Y R, Wang J C, et al. Understanding of the charge storage mechanism of MnO_2-based aqueous zinc-ion batteries: Reaction processes and regulation strategies[J]. Journal of Energy Chemistry, 2023, 82: 423-463.

[12] Liu F, Fan Z. Defect engineering of two-dimensional materials for advanced energy conversion and storage[J]. Chemical Society Reviews, 2023, 52(5): 1723-1772.

[13] Jia H, Li Y, Fu L, et al. Ion Pre-Embedding Engineering of δ-MnO_2 for Chemically Self-Charging Aqueous Zinc Ions Batteries[J]. Small, 2023, 19(46): 2303593.

[14] Hou X, Liu X, Wang H, et al. Specific countermeasures to intrinsic capacity decline issues and future direction of LiMn2O4 cathode[J]. Energy Storage Materials, 2023,57:577-606.

[15] Wang J, Liu Y, Hou Z, et al. Engineering Antibonding Orbital Occupancy for Enhanced Sodium-Ion Intercalation Kinetics in Transition Metal Oxides[J]. Advanced Functional Materials, 2024: 2316719.

[16] Luo S, Zhao X, Qu Y, et al. Insights into the full cycling of oxygen in VOCs oxidation on α-MnO2: A NAP-XPS study[J]. Applied Surface Science, 2023, 634: 157506.

6 Acknowledgments and statement

6.1 Project background and topic selection

With the continuous growth of energy demand and consumption of fossil fuels, the scale of new energy development and application is significantly increasing. Energy storage technology is one of the key technologies to support large-scale development of new energy and increased renewable energy consumption. As an energy storage device with high power density, good low-temperature performance and high safety, supercapacitors play an important role in large-scale energy storage, wearable devices and military fields. Although they are irreplaceable in the field of short-term power compensation when applied to large-scale energy storage systems, supercapacitors suffer from low energy density. As the key material for energy storage of supercapacitors, electrodes are widely studied to improve the performance of supercapacitors.

Manganese dioxide (MnO_2) has been regarded as one of the ideal electrode materials for various energy storage devices such as Zn^{2+}, Na^+ batteries and supercapacitors due to its rich resources, low cost and high theoretical capacity. However, the main problem faced by MnO_2 is the poor cycle stability. Structural distortion and Mn dissolution occur during the charge and discharge process when MnO_2 as electrode material, resulting in serious capacity attenuation and low cycle life. Although many efforts have been performed to address the issue, it is still remaining a significant challenge. Therefore, it is highly desirable to develop a strategy that suppress the structure distortion and Mn dissolution. For addressing this issue, I select this topic.

The strategy is inspired by my hobby in astrophysics and my concern for the universe system. Considering the entire universe system maintains its own stability due to the balance of gravity in the system, the stability of Mn and the coordination atoms in MnO_2 can be regarded as a universe system. It can be inferred that the nature of Mn leaving

this system and dissolving in the electrolyte is due to the broken bond of fixing Mn. Therefore, it may be an effective approach to maintain a strong bonding for Mn atom in MnO_2, that is, strengthening the chemical bond energy connected to Mn can suppress the structure collapse and Mn dissolution. From the periodic table of elements, I found the radius of F element is close to that of O and F possess a relatively strong electronegativity. It is expected that the addition of F with a strong ability to attract electrons can greatly improve the electronic structure and thus improve the chemical bond energy.

6.2 Contributions of instructor and participating student

Thanks for the guidance and supervision of Professor Zhiyu Yang. This project is supervised by Associated Professor Zhiyu Yang at Beijing University of Chemical Technology. Professor Zhiyu Yang has been engaged in research on material chemistry and electrochemistry. At the initial stage of this research project, Professor Yang guided the reading of literature. During the progress of the project, he provided guidance on theoretical and experiments works. At the later stage of the project, he revised the paper.

The above guidance work is unpaid.

Hongyi Li, a student of The High School Affiliated to Renmin University of China, who was responsible for proposing the strategy of this project, literature reviewing, materials synthesis, characterization of materials structure and composition, electrochemical performance testing, DFT calculation, data analysis and the first draft writing of the report.

6.3 Other supports

This work is supported by the Electro-Energy Materials and Technology Laboratory. In the early stage of participating in another research topic of $Na_{0.67}MnO_2$, thanks to the help and guidance of Yuanming Liu during the experiment, which provided an experiments basis for me to finish this research topic successfully.

致谢和说明

课题背景和选题

随着能源需求的持续增长和化石能源的不断消耗，新能源开发和应用规模在不断扩大。储能技术是支持大规模发展新能源产业、提高可再生能源消纳比例、保障能源安全的关键技术之一。超级电容器作为一种功率密度高、低温表现良好和安全性高的储能器件，在大规模储能、可穿戴设备和移动终端等领域，都有重要的应用。比如，在电网出现暂态扰动或功率突变时实现快速功率响应和灵敏调控、主动抑制电网谐波和电压暂降，助力电网运行更加安全可靠；或者，在可穿戴领域，作为一种具有高功率密度的电化学储能设备，特别适用于驱动柔性智能电子设备。然而，以上领域的应用需求给超级电容器带来发展机遇的同时，对其储能能力也提出了巨大的挑战。超级电容器目前主要存在的问题是能量密度偏低，虽然在应用于大规模储能系统实现短时间功率补偿领域无可替代，但在持续性方面还有一定的不足。电极作为超级电容器储能的关键材料，是众多研究者着重关注的超级电容器性能研究领域。

二氧化锰（MnO_2）资源比较丰富、成本低、理论容量高，是最常见的锰系氧化物，被认为是应用于Zn^{2+}、Na^{+}电池和超级电容器等多种储能器件比较理想的电极材料之一。然而，MnO_2面临的一个主要问题是循环稳定性差，在充放电过程中出现结构畸变和Mn溶解，造成容量严重衰减，导致其循环寿命较低。为了解决MnO_2电极材料循环稳定性低的问题，文献工作提出了多种改进性能的方法，但截至目前，MnO_2电极材料电极稳定性低的问题仍然没有解决，成为其产业化应用的一个瓶颈。找到解决MnO_2电极材料稳定性低的方法，构筑超长循环寿命的MnO_2电极材料是一个具有重要科学和实际意义的课题。因此，我选择了这个课题。

策略的提出源于我对天体物理的爱好和对宇宙系统关注的启发。我们知道，整个宇宙系统维持着自己的稳定，是由于系统中引力的平衡。联想到二氧化锰的原子和电子世界，如同一个宇宙系统。Mn离开这个系统溶解于电解液中，是由

于束缚它的化学键断裂，失去将其固定于这个系统中的引力。因此，如果能够让Mn原子在系统中保持大的吸引力，也就是加强和Mn连接的化学键的能量，也许是能够抑制Mn溶解的一个有效方法。从元素周期表中，我找到和半径和O接近，且电负性比较强的F元素，期望对电子吸引能力较强的F的加入，能够较大程度上改善电子结构从而改善化学键键能。

指导老师和参赛学生贡献

杨志宇老师，北京化工大学副教授，从事材料化学和电化学方面的研究，杨老师的研究主要集中在锰氧化物的电化学储能方面。课题研究初期，杨老师指导了我的文献的阅读；课题研究过程中，杨老师指导了理论计算和实验的完成；课题后期，杨老师又对论文的撰写进行了指导和修改。非常感谢杨志宇老师对我的帮助和课题研究的指导！

上述指导工作均无报酬。

李弘毅，人大附中学生。提出了本课题的策略，并负责围绕课题进行文献调研、材料制备、结构和组分的表征、电化学性能测试，理论计算、数据分析和论文初稿的撰写。

其他支持

这项工作得到了北京化工大学电能源材料与技术实验室的支持。前期在另外一个关于$Na_{0.67}MnO_2$材料研究课题的参与过程中，得益于刘袁鸣师兄在实验过程中的帮助和指导，为本课题研究的顺利进行提供了基础。